

## Inhibition Effect of 3D Nanostructures on the Corrosion Resistance of 1-Dodecanethiol Self-Assembled Monolayers on Copper in NaCl Solution

Shuai Hu<sup>1</sup>, Zhenyu Chen<sup>1,2</sup>, Xingpeng Guo<sup>1,2\*</sup>

1. *Key Laboratory for Material Chemistry of Energy Conversion and Storage, Ministry of Education, School of Chemistry and Chemical Engineering, Huazhong University of Science and Technology Wuhan 430074, China*
2. *Hubei Key Laboratory of Materials Chemistry and Service Failure, School of Chemistry and Chemical Engineering, Huazhong University of Science and Technology, Wuhan 430074, China*

**Abstract:** A novel and simple method to improve the corrosion resistance of copper by constructing a 3D 1-dodecanethiol self-assembled monolayers (SAMs) in 3.5% NaCl solution is reported in this study. Several drops of 1% H<sub>3</sub>PO<sub>4</sub> solution are thinly and uniformly distributed on copper surface to form a 3D nanostructure constituted by Cu<sub>3</sub>(PO<sub>4</sub>)<sub>2</sub> nanoflowers. The anticorrosion properties of 1-dodecanethiol SAMs on copper surface and on copper surface treated with H<sub>3</sub>PO<sub>4</sub> solution were evaluated. Results demonstrated that 1-dodecanethiol SAMs on bare copper surface exhibit good protection capacity, whereas a copper surface pretreated with H<sub>3</sub>PO<sub>4</sub> solution can substantially enhance the corrosion resistance of 1-dodecanethiol SAMs.

**Key words:** Copper; Phosphoric acid; 3D Nanostructures; 1-dodecanethiol SAMs

---

\* Corresponding author. Tel: +86-27-87543432; Fax: +86-27-87543632.  
E-mail: [guoxp@hust.edu.cn](mailto:guoxp@hust.edu.cn)

## 1. Introduction

Copper is widely used in microelectronic packaging due to its advantages, such as high electrical and thermal conductivities, low cost, and ease of manufacture [1]. Nevertheless, copper readily undergoes corrosion in practice.

In general, organic compounds containing nitrogen, oxygen, and sulfur, such as benzotriazole [2, 3], 2-mercaptobenzothiazole [4], and 2-mercaptobenzimidazole [5], are frequently used as corrosion inhibitors for copper. In addition, self-assembled monolayers (SAMs) are widely used as barriers to protect copper against corrosion. These compact layers are constituted by highly ordered molecules and formed spontaneously by chemisorption on metal surface. Self-assembly has been recognized as a prospective technology for creating functional materials owing to the extended and two-dimensional molecule layers that can provide excellent corrosion resistance and surface superhydrophobicity [6-8]. Compared with the traditional corrosion inhibition methods, SAMs exhibit the advantages of high coverage, few defects, and high inhibition efficiency [9, 10]. Yamamoto et al. [11] reported that copper with alkanethiol self-assembled layers obtained excellent anticorrosion abilities. Alkanethiols were chemisorbed on the copper surface by covalent linking between Cu and S atoms, forming densely-packed, hydrophobic monolayers on the surface. Zhang et al. [12] studied the inhibition effect of Schiff base SAMs on copper. The maximum inhibition efficiency reached 93.9% for CO<sub>2</sub>-saturated simulative oilfield water after a 3 h self-assembly. Zhang et al. [13] revealed that ammonium pyrrolidine dithiocarbamate SAMs was a mixed-type inhibitor for copper in 3% NaCl solution

and sulfur atoms acted as the active adsorption sites during the self-assembly.

Reportedly, the protective properties of SAMs are closely related to thickness and chain length. Laibinis et al. [8] firstly reported that thicker SAMs retarded the oxidation of copper more obviously than thinner SAMs, and an increase in SAM thickness by about 6 Å led to a corresponding decrease in the rate of oxidation by around 60%. Furthermore, Itoh et al. [14] demonstrated that further chemical modification of an 11-mercapto-1-undecanol SAMs with alkyltrichlorosilanes improved the protective capability of monolayers against corrosion in aqueous and atmospheric environments. The anodic process of corrosion was inhibited by network structures owing to two-dimensional polymerization with lateral siloxane linkage between molecules absorbed on copper.

In addition, electro-assisted methods, such as direct-current and alternation-current treatments, have been applied to further optimize self-assembled films [15-17]. Wang et al. [17] reported a novel method for fabricating an effective inhibition film on copper. Phenylthiourea was absorbed in a copper surface, 1-dodecanethiol was used for subsequent modification, and alternating-current voltage was applied on copper covered with the mixed film for further modification.

Structures and compositions of the metal surface markedly affect the protective property of SAMs. Inhomogeneity and instability of the metal substrate typically result in disordered adsorption layers and poor anticorrosion capability. Rohwerder et al. [18] reported that clean metal surface and metal surface covered with stable oxides were more beneficial for self-assembly than metal surface covered with unstable

oxides.

To date, few papers have reported on the effect of surface composition and structure on SAMs for the corrosion inhibition of copper. In this paper, the preliminary goal is the fabrication of stable nanostructures on the copper surface. According to previous research, several methods of constructing nanostructures on the copper surface were established. For example, Wang et al. [19] obtained desirable 3D nanostructures on copper surface by immersing copper in  $\text{H}_3\text{PO}_4$  solution. Structure and chemical composition were tunable by simply changing the concentration of  $\text{H}_3\text{PO}_4$  solution and immersion time. He et al. [20] reported the  $\text{Cu}_3(\text{PO}_4)_2$  nanoflowers were formed through the interfacial reaction between copper foil and phosphate-buffered saline and found that the formation of nanoflowers was related to the concentration of dissolved oxygen, chloride ions, and phosphate ions.

Herein, we reported a simple method for improving the corrosion resistance of SAMs on copper via a pretreatment method using  $\text{H}_3\text{PO}_4$  solution. 1-Dodecanethiol was selected for the formation of SAMs. The copper surface was characterized using scanning electron microscopy (SEM), X-ray photoelectron spectroscopy (XPS), and X-ray diffraction (XRD). The corrosion resistance of 1-dodecanethiol SAMs on  $\text{H}_3\text{PO}_4$ -treated copper surface was studied by using potentiodynamic polarization curves and electrochemical impedance spectroscopy (EIS).

## **2. Experimental**

### *2.1 Materials and solutions*

Working electrodes were prepared from a copper sheet of purity 99.9%. For

electrochemical studies, copper specimens were embedded in epoxy resin, with a surface area of 1 cm<sup>2</sup> exposed to the electrolyte. The surface of the samples were initially ground with 400-grit emery paper and continued with 800- and 1200-grit emery papers successively. Then the samples were washed with distilled water, degreased with ethanol and acetone, and finally dried with a flow of nitrogen gas.

1-Dodecanethiol (C<sub>12</sub>H<sub>25</sub>SH) from Aladdin with ≥ 98% purity was dissolved in absolute ethanol (AR grade) to a concentration of 80 g/L. An aqueous solution of 3.5% NaCl solution was prepared by dissolving NaCl (AR grade) in double-distilled water. H<sub>3</sub>PO<sub>4</sub> (AR grade, ≥ 85%) concentrated solution was diluted to a concentration of 1%, and the pH value of the solution was adjusted to 2.5 by using NaOH solution.

### *2.2 Fabricating 3D nanostructures on copper surface*

Several drops of 1% H<sub>3</sub>PO<sub>4</sub> solution were uniformly spread on the copper surface to form an ultrathin liquid membrane. Fresh H<sub>3</sub>PO<sub>4</sub> solution was added to maintain the liquid membrane during the process. After 1 h, the sample was immersed in distilled water for 2 min to terminate the reaction. The temperature was controlled at 25 °C during preparation.

### *2.3 Formation of 1-dodecanethiol SAMs*

The samples (copper and copper treated with H<sub>3</sub>PO<sub>4</sub> solution) were dried in a vacuum dryer for 12 h to thoroughly remove water on the surface. The SAMs were formed by immersing the samples in 1-dodecanethiol ethanol solution for 3 h. Then the samples were washed with flowing distilled water and dried under nitrogen gas flow.

## 2.4 Characterization

Surface morphologies were obtained via scanning electron microscopy (SEM, Phillips Quanta 200) coupled with energy dispersive X-ray spectroscopy (EDS). XPS spectra were measured using a commercial VG Multilab 2000 system. An Al K $\alpha$  radiation source (1486.6 eV) was equipped for the spectrum measurements, and the electron energy resolution was 0.45 eV. Spectral decomposition was performed using background subtraction and a least-squares fitting program. XRD measurement was conducted on an Empyrean X-ray diffractometer from PANalytical (a Cu K $\alpha$  irradiation source,  $\lambda=1.5418$  Å). The FTIR spectrum of H<sub>3</sub>PO<sub>4</sub>-treated copper surface with 1-dodecanethiol SAMs was recorded using a Bruker VERTEX 70 Fourier transform infrared spectrophotometer within a range of 4000 cm<sup>-1</sup> to 400 cm<sup>-1</sup>. The infrared spectra of pure 1-dodecanethiol and copper surface treated with H<sub>3</sub>PO<sub>4</sub> solution were measured for comparison.

Contact angle measurements were carried out for the wettability evaluations of copper surface. A small water droplet was placed on the surface by using the microsyringe and the volume was controlled at 2  $\mu$ L. The contact angle was determined by averaging the values obtained from three positions of each sample.

## 2.5 Electrochemical measurements

Electrochemical measurements were conducted using an IM6e electrochemical workstation in a conventional three-electrode cell with 3.5% NaCl solution. Potentiodynamic polarization curves were obtained at a sweep rate of 0.5 mV/s in the potential range of -250 mV to +800 mV versus the open circuit potential. EIS

measurements were conducted at the open circuit potential with a 10-mV amplitude perturbation at frequencies from 100 kHz to 10 mHz, with 10 points per decade. Impedance data were fitted to the appropriate equivalent circuits by using Zview software. All potential values in this paper refer to the saturated calomel electrode (SCE).

### 3. Results

#### 3.1 Surface Characterization

##### 3.1.1 SEM surface morphologies

Fig. 1 presents the SEM pictures and EDS mapping for copper surface, (a, b) treated with  $\text{H}_3\text{PO}_4$  solution, (c) with 1-dodecanethiol SAMs, and (d, e, f) with  $\text{H}_3\text{PO}_4$  solution and modified with 1-dodecanethiol SAMs. In Fig. 1a, the copper surface is overspread with densely-packed flower-like nanostructures. In Fig. 1b, the sheet structures of the free-standing  $\text{Cu}_3(\text{PO}_4)_2$  nanoflower can be observed clearly. Given that the surface was densely packed with these nanosheets, a 3D network full of channels and cavities was formed. Fig. 1c shows the bare copper surface with 1-dodecanethiol SAMs. In Figs. 1(d) and 1(e), the self-assembly of 1-dodecanethiol SAMs on  $\text{H}_3\text{PO}_4$ -treated copper surface caused the formation of a mass of thick fragments distributed among the nanoflowers. According to the EDS mapping of the  $\text{H}_3\text{PO}_4$ -treated copper surface with 1-dodecanethiol SAMs, the outline of the nanoflowers were observed clearly, and the chemical composition of the fragment is mainly C and S, which indicates that the fragments contain numerous 1-dodecanethiol molecules.

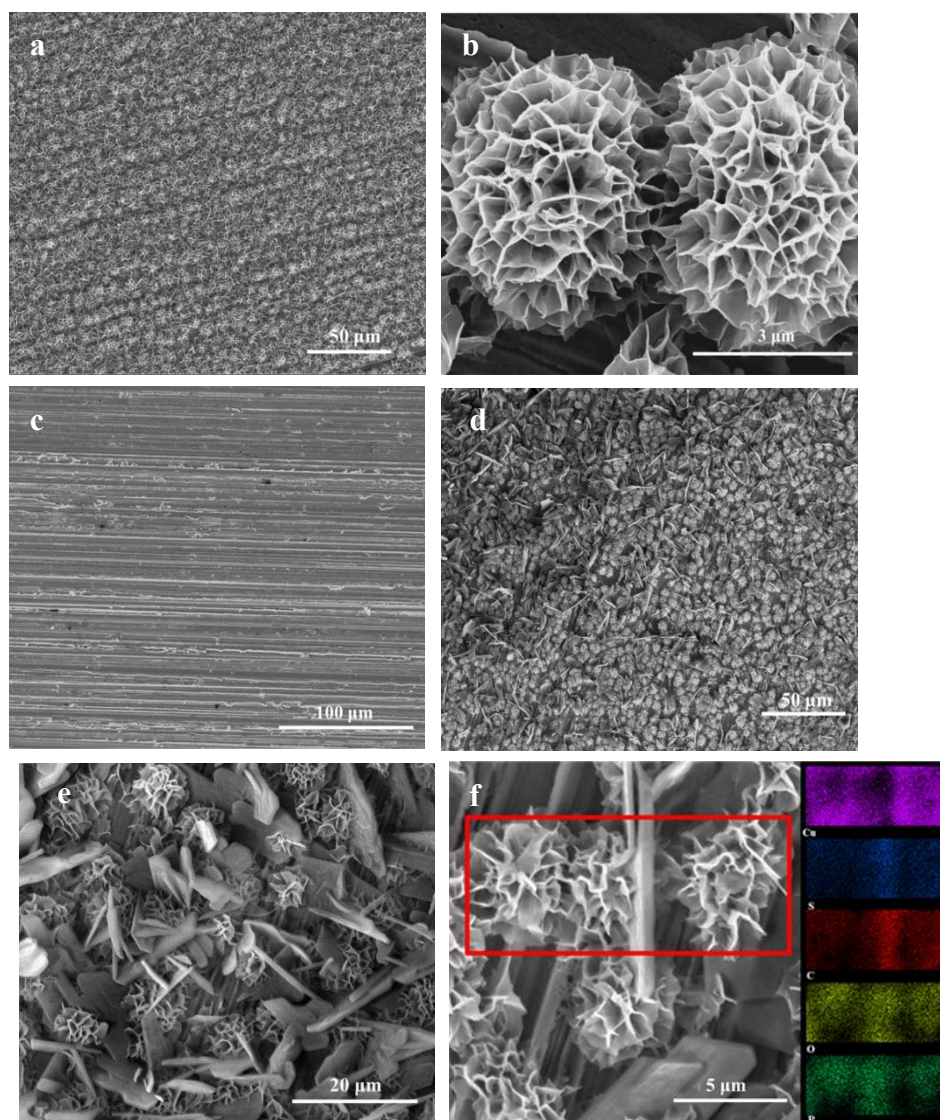


**Fig. 1** SEM images of (a, b) copper surface treated with  $H_3PO_4$  solution; (c) copper surface with 1-dodecanethiol SAMs; (d, e) copper surface-reated with  $H_3PO_4$  solution and modified with 1-dodecanethiol SAMs; (f) EDS mapping

### 3.1.2 XPS analysis

XPS analyses were carried out to determine the chemical composition of the copper surface. Fig. 2a shows the XPS spectra of  $H_3PO_4$ -treated copper surface with 1-dodecanethiol SAMs. The deconvolution spectra for C, Cu, O, P, and S are shown in Figs. 2b–2f. The peak at 284.7 eV can be attributed to organic carbon in the system [21]. A weak peak at 935.1 eV, which is characteristic of  $Cu_3(PO_4)_2$ , was overlapped

by the strong Cu  $2p_{3/2}$  peak corresponding to Cu(I) or Cu(0) [22, 23]. The XPS spectra of O 1s core level that deconvoluted into two components were located at 531.0 and 532.0 eV, which correspond to copper oxides and phosphate, respectively [24, 25]. The peak at 133.6 eV in P 2p spectrum is attributed to P  $2p_{1/2}$  of  $\text{Cu}_3(\text{PO}_4)_2$  [23]. The binding energy of S peak for 1-dodecanethiol absorbed on copper is 162.2 eV, indicating that 1-dodecanethiol chemisorbed on the surface by thiolate formation, whereas the peak at 163.3 eV can be attributed to the 1-dodecanethiol molecule [26].

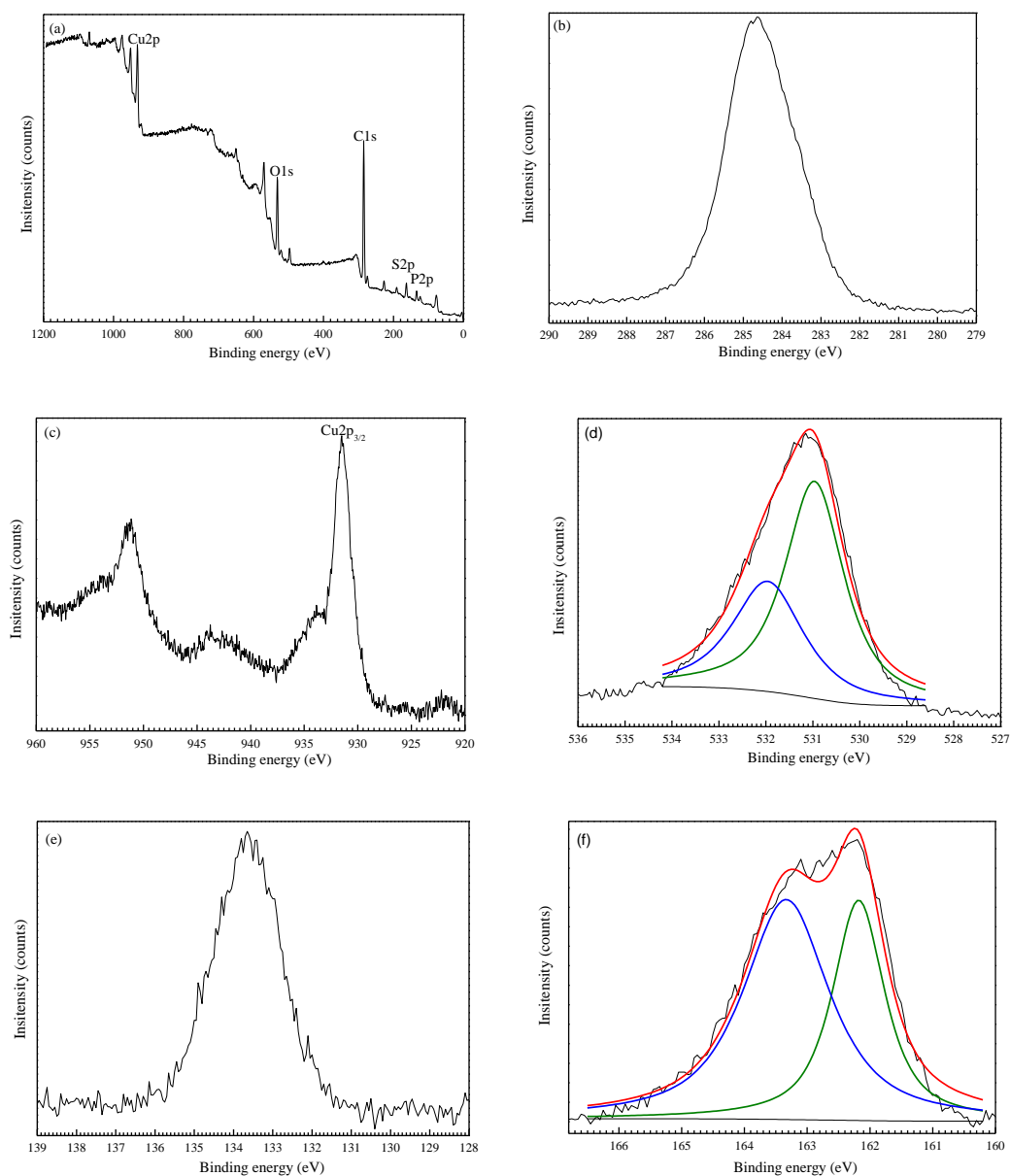


**Fig. 2** XPS spectra of major elements on copper surface treated with H<sub>3</sub>PO<sub>4</sub> solution and modified with 1-dodecanethiol SAMs (a) XPS, (b) C 1s, (c) Cu 2p, (d) O 1s, (e) P 2p, and (f) S 2p

Furthermore, surface analyses were implemented on the copper surface treated with H<sub>3</sub>PO<sub>4</sub> solution and bare copper surface with 1-dodecanethiol SAMs; the corresponding quantification (%) of each element are summarized in Table 1. Compared with the chemical composition of bare copper surface with 1-dodecanethiol SAMs, the contents of elements C and S evidently increased for the H<sub>3</sub>PO<sub>4</sub>-treated copper surface with 1-dodecanethiol SAMs. The results indicated that the copper surface absorbed additional 1-dodecanethiol molecules when pretreated using H<sub>3</sub>PO<sub>4</sub> solution.

**Table 1** The atomic ratios (%) of elements on detected samples

	C	Cu	O	P	S
Cu/H <sub>3</sub> PO <sub>4</sub>	73.25	8.19	14.36	4.19	-
Cu/1-dodecanethiol	75.07	15.31	7.58	-	2.03
Cu/H <sub>3</sub> PO <sub>4</sub> /1-dodecanethiol	81.19	5.01	3.51	3.61	6.67

### 3.1.3 XRD measurement

The XRD pattern of the nanoflower is shown in Fig. 3, and several peaks at 8.9°, 12.8°, and 29.5° match well with Cu<sub>3</sub>(PO<sub>4</sub>)<sub>2</sub>·3H<sub>2</sub>O [JCPDS card 00-022-0548] [27]. These results revealed that the copper surface was covered with copper phosphate after H<sub>3</sub>PO<sub>4</sub> solution treatment.

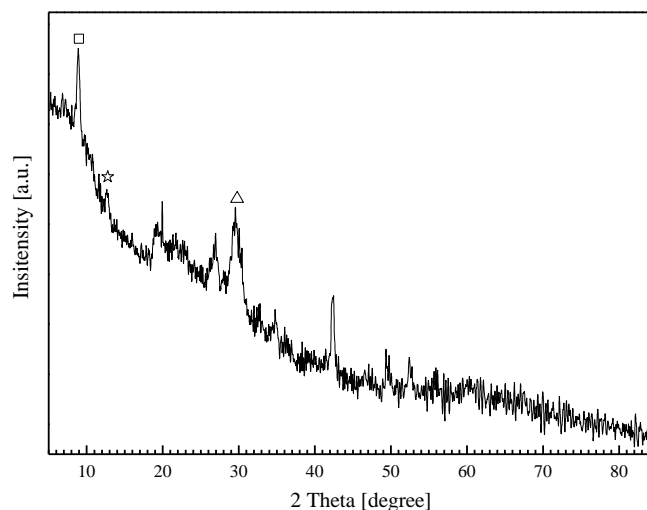


**Fig. 3** XRD pattern of Cu<sub>3</sub>(PO<sub>4</sub>)<sub>2</sub> nanoflower

#### 3.1.4 FTIR measurements

The FTIR spectra of copper surface treated with H<sub>3</sub>PO<sub>4</sub> solution, pure 1-dodecanethiol, and copper surface treated with H<sub>3</sub>PO<sub>4</sub> solution and modified with 1-dodecanethiol SAMs are shown in Fig. 4. The bands that appeared around 1625 cm<sup>-1</sup> may be due to the absorbed water of Cu<sub>3</sub>(PO<sub>4</sub>)<sub>2</sub> nanoflowers [20]. In Fig. 4a, the bands at 1060 and 992 cm<sup>-1</sup> correspond to the asymmetric and symmetric stretching vibrations of PO<sub>4</sub><sup>3-</sup> ions. The bands at 629 and 560 cm<sup>-1</sup> are due to the out-of-plane bending vibrations of PO<sub>4</sub><sup>3-</sup> ions [20, 28]. In Fig. 4b, the band at 2956 cm<sup>-1</sup> is assigned to the asymmetric stretching vibration of CH<sub>3</sub>. The bands at 2924 and 2853 cm<sup>-1</sup> can be ascribed to the asymmetric and symmetric stretching vibrations of CH<sub>2</sub>, respectively [29]. The bands at 1464 and 722 cm<sup>-1</sup> correspond to the bending vibration of S-CH<sub>2</sub> and stretching vibration of S-C, respectively. Although slight shifts of these wave numbers occurred due to the disordered conformation of alkyl chains were observed, the result was in good agreement with those of C<sub>5</sub>-C<sub>21</sub> alkanethiol SAMs absorbed on gold [30, 31]. The bands in Fig. 4c match well with

those in Figs. 4a and 4b, indicating that 1-dodecanethiol molecules were strongly absorbed on  $\text{H}_3\text{PO}_4$ -treated copper surface.

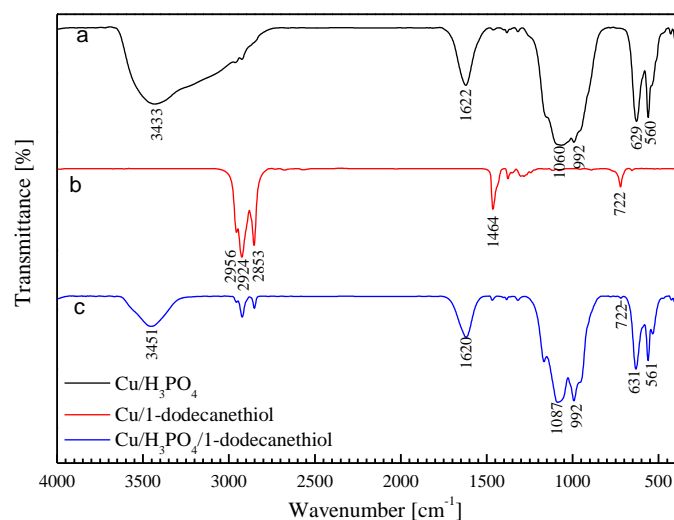


**Fig. 4** FTIR spectra of (a) copper surface treated with  $\text{H}_3\text{PO}_4$  solution, (b) pure 1-dodecanethiol, and (c) copper surface treated with  $\text{H}_3\text{PO}_4$  solution and modified with 1-dodecanethiol SAMs

### 3.1.5 Contact angle measurements

The wettability of 1-dodecanethiol SAMs was tested by measuring the contact angle, which is closely linked to the adsorption molecules and properties of the solid surface, such as surface energy and surface roughness [32]. When the head of 1-dodecanethiol molecules were absorbed on the copper surface, densely-packed long alkyl chains were oriented towards the solution, resulting in a hydrophobic surface and increased contact angle. Fig. 5 shows the water drop on the bare copper surface, copper surface with 1-dodecanethiol SAMs, and  $\text{H}_3\text{PO}_4$ -treated copper surface with 1-dodecanethiol SAMs. The bare copper surface exhibited hydrophilicity with a water contact angle of approximately  $91.5^\circ$ , whereas that on copper surface with 1-dodecanethiol SAMs was  $127^\circ$ , and that on  $\text{H}_3\text{PO}_4$ -treated copper surface with 1-dodecanethiol SAMs was  $125^\circ$ . These results demonstrated that the copper surface

with 1-dodecanethiol SAMs became hydrophobic, and the pre-treatment on copper surface with  $H_3PO_4$  solution minimally affected wettability.

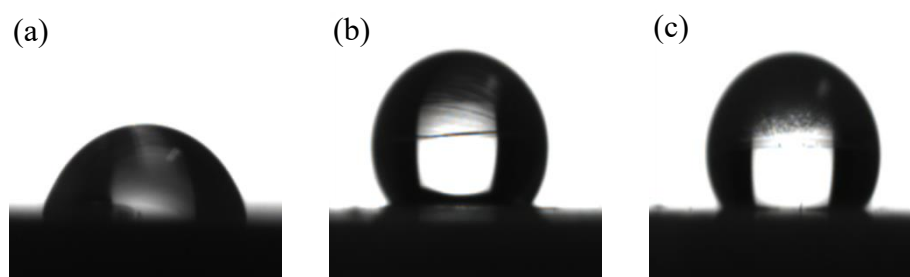


**Fig. 5** Contact angle of water droplets on (a) bare copper surface, (b) copper surface with 1-dodecanethiol SAMs, and (c)  $H_3PO_4$ -treated copper surface with 1-dodecanethiol SAMs

### 3.2 Anticorrosion investigations of 1-dodecanethiol SAMs

#### 3.2.1 Potentiodynamic polarization measurements

Fig. 6 shows the potentiodynamic polarization curves obtained in 3.5% NaCl solution for bare copper electrode, copper electrode with 1-dodecanethiol SAMs, and  $H_3PO_4$ -treated copper electrode with 1-dodecanethiol SAMs.

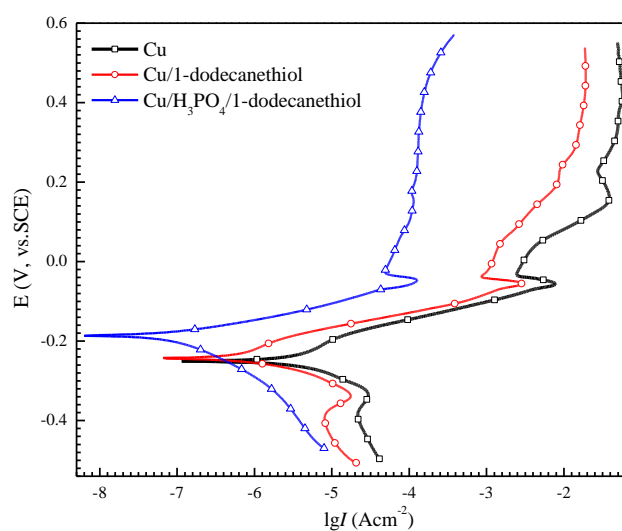


**Fig. 6** Potentiodynamic polarization curves obtained in 3.5% NaCl solution after 48 h for bare copper electrode, copper electrode with 1-dodecanethiol SAMs, and copper electrode treated with  $H_3PO_4$  solution and modified with 1-dodecanethiol SAMs

The anodic reactions are generally considered reversible. The kinetics and

mechanisms in the neutral NaCl solution are as follows:



The typically anodic polarization curves for bare copper in neutral NaCl solution can be illuminated by dividing the curves into three parts according to the potential region [33]. Section I: From the Tafel region to the maximum current density. Section II: a region of the current density decreased to the minimum. Section III: a region of increasing in current density to the limited value. The increase in current density at Section I was due to the oxidation of copper to the cuprous ion. With the increase in potential, the decrease in current density to the minimum resulted from the formation of CuCl film. Then CuCl was transformed to soluble CuCl<sub>2</sub> at higher potentials resulting in a limiting current density. Above the limiting-current region, the increase in current density might be caused by the formation of Cu(II) species. This phenomenon was also observed in the anodic behaviors of both electrodes modified with 1-dodecanethiol SAMs. Moreover, the cathodic reaction can be related to the reduction of hydrogen ion or dissolved oxygen. Given that the equilibrium potential for hydrogen evolution in a solution at pH 7 is -662 mV versus SCE, the occurrence of hydrogen ion reduction is impossible. Correspondingly, the reduction potential of oxygen is 568 mV versus SCE, indicating that the reduction of oxygen is thermodynamically possible [34]. A small hump appeared on the cathodic curves for

bare copper electrode and copper electrode with 1-dodecanethiol SAMs at a potential around  $-300$  mV versus SCE, which may be caused by the reduction of CuCl and/or Cu<sub>2</sub>O [35-37].

As seen from this image, the corrosion rate of bare copper electrode with 1-dodecanethiol SAMs was effectively decreased. By contrast, the corrosion rate of H<sub>3</sub>PO<sub>4</sub>-treated electrode with 1-dodecanethiol SAMs unexpectedly decreased by one order of magnitude. In addition, the corrosion potential of the H<sub>3</sub>PO<sub>4</sub>-treated electrode with 1-dodecanethiol SAMs notably shifted to a positive region. The corresponding electrochemical results, such as corrosion potential ( $E_{\text{corr}}$ ), Tafel slope ( $b_a$ ,  $b_c$ ), and corrosion current density ( $i_{\text{corr}}$ ), are summarized in Table 2. Inhibition efficiency (IE%) were calculated using the following equation:

$$\text{IE}\% = \frac{i_{\text{corr}} - i'_{\text{corr}}}{i_{\text{corr}}} \times 100 \quad (5)$$

where  $i_{\text{corr}}$  and  $i'_{\text{corr}}$  are the corrosion current densities of bare copper electrode and electrodes with 1-dodecanethiol SAMs in 3.5% NaCl solution, respectively. The inhibition efficiency increased from 73.1% to 97.2% when the electrode was processed with H<sub>3</sub>PO<sub>4</sub> solution, which indicated that H<sub>3</sub>PO<sub>4</sub> treatment of the copper surface prior to self-assembly is favorable for corrosion protection.

**Table 2** Polarization parameters of copper electrode, copper electrode with 1-dodecanethiol SAMs and H<sub>3</sub>PO<sub>4</sub>-treated copper electrode with 1-dodecanethiol SAMs in 3.5% NaCl solution for 48 h

	$E_{\text{corr}}$ (mV)	$b_a$ (mV/dec)	$b_c$ (mV/dec)	$i_{\text{corr}}$ (A/cm <sup>2</sup> )	IE%
Cu	-247	97	-66	$4.75 \times 10^{-6}$	-
Cu/1-dodecanethiol SAMs	-235	199	-49	$1.28 \times 10^{-6}$	73.1

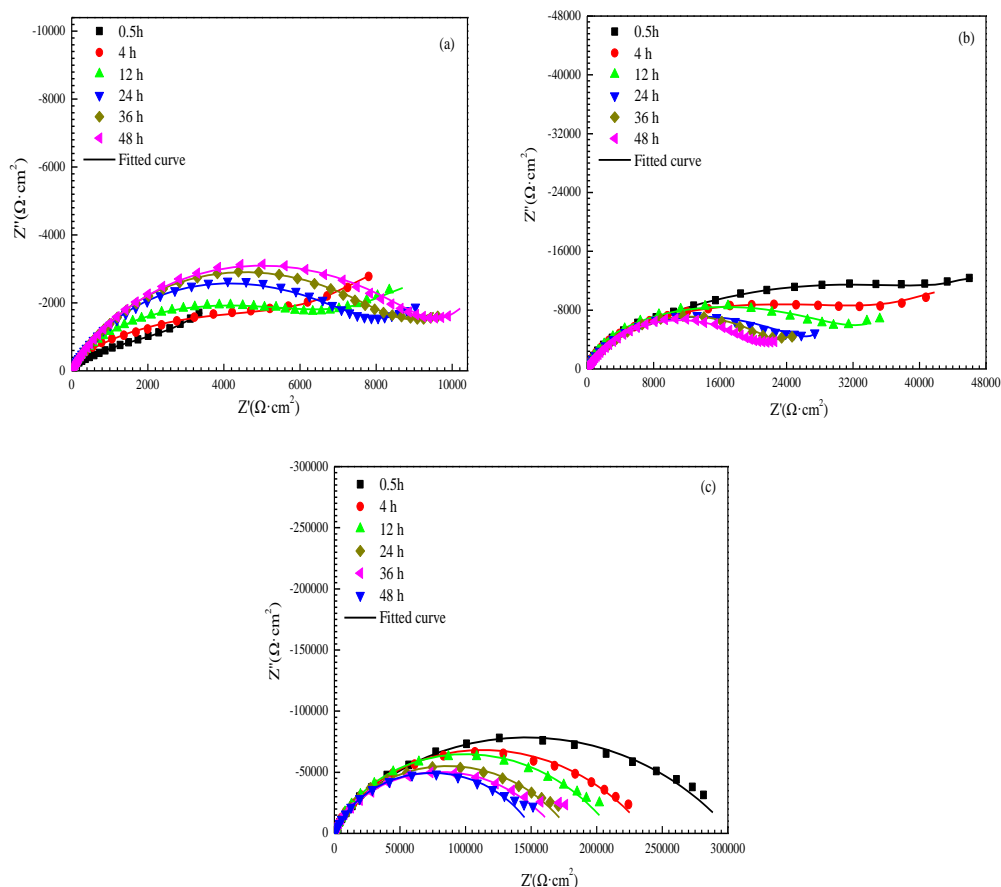
---

Cu/H <sub>3</sub> PO <sub>4</sub> /1-dodecanethiol SAMs	-187	48	-205	1.32×10 <sup>-7</sup>	97.2
---	------	----	------	-----------------------	------

---

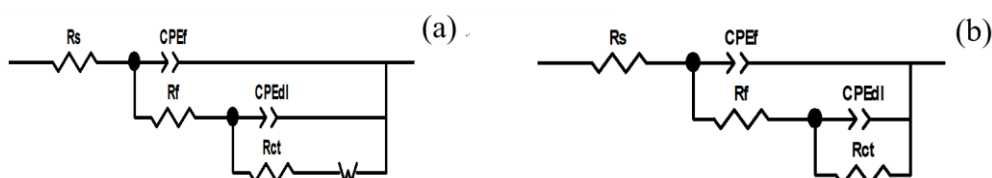
### 3.2.2 EIS measurements

Fig. 7 shows the EIS of bare copper electrode, copper electrode with 1-dodecanethiol SAMs, and H<sub>3</sub>PO<sub>4</sub>-treated copper electrode with 1-dodecanethiol SAMs in 3.5% NaCl solution for different times. The Nyquist plot of the bare copper electrode and copper electrode with 1-dodecanethiol SAMs displayed a depressed semicircle at high frequency and a straight line in the low frequency region was observed. The high-frequency semicircle could be attributed to the charge-transfer process, and the low-frequency linear portion, namely, Warburg impedance was the result of anodic diffusion of soluble CuCl<sub>2</sub><sup>-</sup> from the electrode/ electrolyte interface to the bulk solution or the reduction of dissolved oxygen controlled by the oxygen diffusion [38, 39]. The Warburg impedance in the Nyquist plot indicated that the corrosion of copper was influenced by the mass-transport process to a certain extent. Fig. 7c shows that Warburg impedance disappears when the copper electrode was pre-treated using H<sub>3</sub>PO<sub>4</sub> solution, indicating that corrosion was controlled by the charge-transfer process. The significant increase in the diameter of the arc could be ascribed to a better absorption of 1-dodecanethiol SAMs, suggesting the corrosion resistance was enhanced remarkably.



**Fig. 7** Nyquist plots of (a) bare copper electrode, (b) copper electrode with 1-dodecanethiol SAMs, and (c)  $\text{H}_3\text{PO}_4$ -treated copper electrode with 1-dodecanethiol SAMs in 3.5% NaCl solution

The electrochemical impedance parameters of the bare copper electrode and copper electrode with 1-dodecanethiol SAMs were obtained using the equivalent circuit mode in Fig. 8a, whereas Fig. 8b was used to fit those of the  $\text{H}_3\text{PO}_4$ -treated copper electrode with 1-dodecanethiol SAMs.



**Fig. 8** Equivalent circuits used for fitting impedance data

$R_s$  is the solution resistance,  $R_f$  is the resistance of 1-dodecanethiol SAMs on the copper electrode surface,  $R_{ct}$  represents the charge-transfer resistance, and CPE is the

constant phase element. Given the lack of pure capacitance in the non-ideal electrochemical behavior of the surface, a CPE was used to substitute the pure capacitance. In general, a CPE is applicable to the case of surface inhomogeneity (e.g. electrode roughness and adsorbate) [40]. The impedance of CPE is defined as follows:

$$Z_{\text{CPE}} = [Y(j\omega)^n]^{-1} \quad (6)$$

where  $Y$  is the magnitude of CPE,  $\omega$  is the angular frequency,  $j$  is an imaginary number, and  $n$  is the exponential term represents the degree of the surface inhomogeneity. The corresponding values of these impedance parameters are listed in Table 3.

**Table 3** Electrochemical impedance parameters of bare copper electrode, copper electrode with 1-dodecanethiol SAMs and  $\text{H}_3\text{PO}_4$ -treated copper electrode with 1-dodecanethiol SAMs

	Time (h)	$R_s$ ( $\Omega \cdot \text{cm}^2$ )	$\text{CPE}_f$ ( $\text{S}^n \cdot \Omega^{-1} \cdot \text{cm}^{-2}$ )	$n$	$R_f$ ( $\Omega \cdot \text{cm}^2$ )	$\text{CPE}_{dl}$ ( $\text{S}^n \cdot \Omega^{-1} \cdot \text{cm}^{-2}$ )	$n$	$R_{ct}$ ( $\Omega \cdot \text{cm}^2$ )
Cu	0.5	3	$1.96 \times 10^{-5}$	0.96	81	$2.92 \times 10^{-4}$	0.47	3762
	4	4	$2.62 \times 10^{-6}$	0.98	293	$8.18 \times 10^{-5}$	0.46	7292
	12	4	$4.23 \times 10^{-6}$	0.98	109	$5.98 \times 10^{-5}$	0.51	7533
	24	4	$4.18 \times 10^{-6}$	0.98	137	$4.20 \times 10^{-5}$	0.68	7832
	36	4	$4.04 \times 10^{-6}$	0.95	155	$4.09 \times 10^{-5}$	0.71	8654
	48	4	$3.73 \times 10^{-6}$	0.92	185	$3.51 \times 10^{-5}$	0.69	9625
Cu/ 1-dodecanethiol SAMs	0.5	6	$1.69 \times 10^{-6}$	0.88	6573	$1.93 \times 10^{-5}$	0.47	50575
	4	5	$2.00 \times 10^{-6}$	0.88	6398	$2.04 \times 10^{-5}$	0.45	35949
	12	7	$2.46 \times 10^{-6}$	0.98	4597	$2.17 \times 10^{-5}$	0.50	31803
	24	6	$3.08 \times 10^{-6}$	0.94	3291	$2.23 \times 10^{-5}$	0.53	25286
	36	4	$3.96 \times 10^{-6}$	0.89	1277	$2.32 \times 10^{-5}$	0.65	22670
	48	4	$5.04 \times 10^{-6}$	0.92	931	$2.52 \times 10^{-5}$	0.64	21026
Cu/ $\text{H}_3\text{PO}_4$ / 1-dodecanethiol SAMs	0.5	4	$1.21 \times 10^{-6}$	0.57	1086	$1.04 \times 10^{-7}$	0.88	302811
	4	8	$1.33 \times 10^{-6}$	0.52	429	$9.82 \times 10^{-7}$	0.80	239891
	12	5	$1.41 \times 10^{-6}$	0.52	347	$1.21 \times 10^{-6}$	0.84	214319
	24	5	$1.68 \times 10^{-6}$	0.55	237	$1.54 \times 10^{-6}$	0.82	181316
	36	5	$1.86 \times 10^{-6}$	0.50	202	$1.79 \times 10^{-6}$	0.81	172380
	48	6	$2.15 \times 10^{-6}$	0.60	153	$2.83 \times 10^{-6}$	0.82	153320

As shown in Table 3,  $R_{ct}$  of bare copper increases with immersion time. This trend was relative to the formation of limited protective  $\text{Cu}_2\text{O}$  and  $\text{CuO}$  films [34]. Compared with the bare copper electrode, the formed 1-dodecanethiol SAMs on the bare copper surface considerably increase the  $R_{ct}$  values in the first few hours, indicating that 1-dodecanethiol SAMs on the copper surface effectively inhibited corrosion. Furthermore, pretreatment of the copper electrode with  $\text{H}_3\text{PO}_4$  solution can markedly enhance the corrosion resistance given that the  $R_{ct}$  value is one order of magnitude larger than that of the non-pretreated electrode. Corresponds to the increase of impedance values, the significant decrease in  $\text{CPE}_{dl}$  values for  $\text{H}_3\text{PO}_4$ -treated electrode can be ascribed to the replacement of water molecules by the adsorption of 1-dodecanethiol SAMs on the electrode surface. The decrease in  $R_{ct}$  values with increasing immersion time was observed for both copper electrodes modified with 1-dodecanethiol SAMs. This finding suggests that the 1-dodecanethiol SAMs lose their protective property under continuous attack of dissolved oxygen and chloride ions.

### *3.3 Corrosion behaviors of copper treated with $\text{H}_3\text{PO}_4$ solution*

Figs. 9 and 10 show the potentiodynamic polarization curves and EIS of copper electrode with or without  $\text{H}_3\text{PO}_4$  solution treatment, respectively. Electrochemical measurements were performed after the system was stabilized in  $\text{NaCl}$  solution for 30 min. The corresponding potentiodynamic polarization parameters are listed in Table 4.

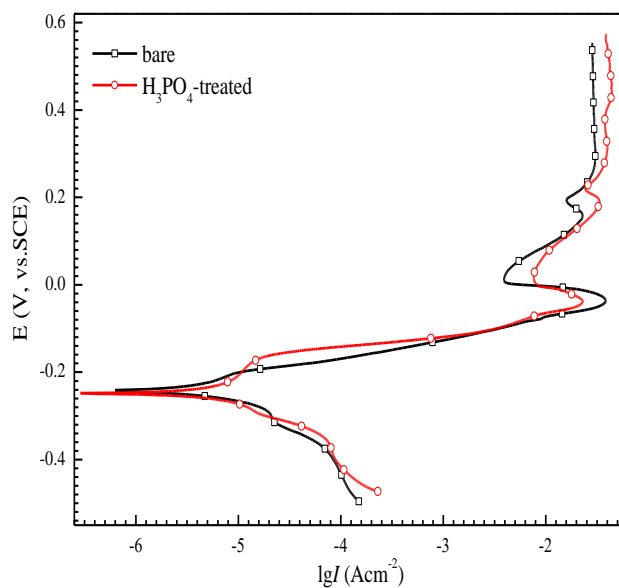


**Fig. 9** Potentiodynamic polarization curves of copper electrode with or without H<sub>3</sub>PO<sub>4</sub> solution treatment

**Table 4** Polarization parameters of copper electrode with and without H<sub>3</sub>PO<sub>4</sub> solution treatment

	$E_{\text{corr}}$ (mV)	$b_a$ (mV/dec)	$b_c$ (mV/dec)	$i_{\text{corr}}$ (A/cm <sup>2</sup> )
Cu	-243	116	-60	$6.60 \times 10^{-6}$
Cu/H <sub>3</sub> PO <sub>4</sub>	-248	98	-66	$7.81 \times 10^{-6}$

Electrochemical impedance parameters were obtained using the equivalent circuit mode in Fig. 8a and are summarized in Table 5. The results showed that the bare electrode showed superior corrosion resistance than H<sub>3</sub>PO<sub>4</sub>-treated electrode. This finding suggests that the 3D nanoflowers on the surface did not improve the corrosion resistance of copper without 1-dodecanethiol SAM modification.

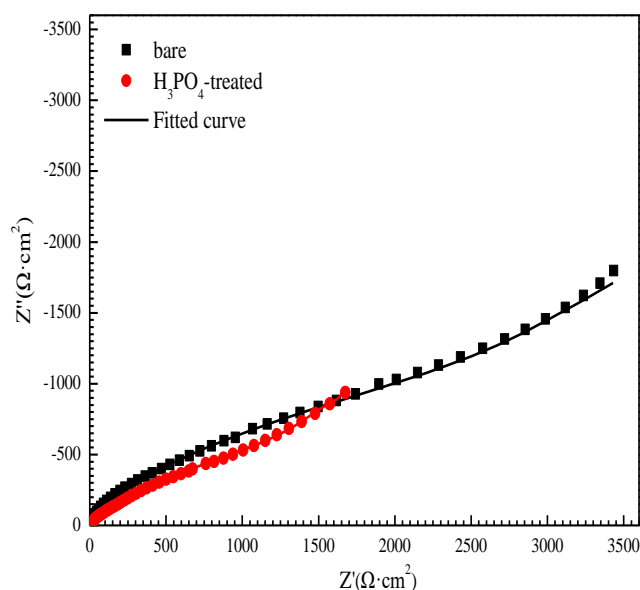


**Fig. 10** Nyquist plots of copper electrode with or without H<sub>3</sub>PO<sub>4</sub> solution treatment

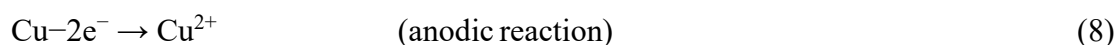
**Table 5** Electrochemical impedance parameters of copper electrode with and without H<sub>3</sub>PO<sub>4</sub>

	solution treatment									
	$R_s$ ( $\Omega \cdot \text{cm}^2$ )	$\text{CPE}_r$ ( $\text{S}^n \cdot \Omega^{-1} \cdot \text{cm}^{-2}$ )	$n$	$R_f$ ( $\Omega \cdot \text{cm}^2$ )	$\text{CPE}_{dl}$ ( $\text{S}^n \cdot \Omega^{-1} \cdot \text{cm}^{-2}$ )	$n$	$R_{ct}$ ( $\Omega \cdot \text{cm}^2$ )	W-R ( $\Omega \cdot \text{cm}^2$ )	W-T ( $\Omega^{-1} \cdot \text{cm}^{-2}$ )	W-P
Cu	3	$1.96 \times 10^{-5}$	0.96	81	$2.94 \times 10^{-4}$	0.47	3762	5515	45	0.48
Cu/H <sub>3</sub> PO <sub>4</sub>	4	$4.64 \times 10^{-5}$	0.87	53	$8.50 \times 10^{-4}$	0.45	2649	5390	90	0.71

#### 4. Discussion

The pretreatment of copper surface with H<sub>3</sub>PO<sub>4</sub> solution is necessary to obtain excellent protective properties. In our previous unsuccessful trials, the H<sub>3</sub>PO<sub>4</sub> solution was placed on the copper surface without spreading, and the nanoflowers were found to grow on the margin of the liquid membrane on the copper surface, whereas nothing was found in the center except certain trails of corrosion. According to these results and those of previous reports [20, 34], the formation of the Cu<sub>3</sub>(PO<sub>4</sub>)<sub>2</sub> nanoflowers is closely linked to the concentration of dissolved oxygen and PO<sub>4</sub><sup>3-</sup> ions. The formation of Cu<sub>3</sub>(PO<sub>4</sub>)<sub>2</sub> nanoflowers is illustrated in Fig. 11, and the corresponding equations are

as follows:



The released  $\text{Cu}^{2+}$  ions react with  $\text{PO}_4^{3-}$  ions immediately, generating a solubilized layer of phosphate complex intermediate. The free phosphoric acid then corrodes the intermediate, resulting in selective crystallization into nanoparticles, which function as nuclei in the subsequent crystallization [19]. As the reactions progress, additional nanosheets are generated and aggregated into a flower-like sphere. Eventually, the surface is covered by the interconnected flower-like nanosheets. During the fabrication of nanoflowers, a paper-thin liquid membrane must be spread uniformly on the surface to ensure sufficient oxygen. Meanwhile, fresh  $\text{H}_3\text{PO}_4$  solution is needed to maintain the liquid membrane and supplement adequate  $\text{PO}_4^{3-}$  ions.

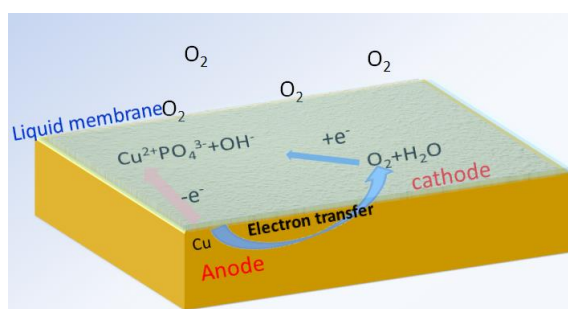


**Fig. 11** Schematic of the formation of  $\text{Cu}_3(\text{PO}_4)_2$  nanoflowers

In the EIS measurements, for the electrodes modified with 1-dodecanethiol SAMs, the values of impedance gradually decreased with time, indicating that 1-dodecanethiol SAMs started to deteriorate with the attack of dissolved oxygen or chloride ions. According to a previous report [41], 1-dodecanethiol SAMs are

sensitive to air exposure, which causes an increase in the density of defects and a decrease in film thickness. The mechanism for deterioration of 1-dodecanethiol SAMs can be ascribed to the oxidation of thiolates to less-adherent sulfonates, leading to the roughening of the copper surface. The rougher surface may distort the structure of the hydrocarbon lattice and increase the permeability of the SAMs [8, 42]. Compared with the bare copper surface, copper surface treated with  $H_3PO_4$  solution exhibited a large 3D network structure that adsorbed and accommodated additional 1-dodecanethiol molecules. Correspondingly, the 2D 1-dodecanethiol SAMs on the bare copper was turned into 3D SAMs. The interconnected nanosheets modified with 1-dodecanethiol monolayers constructed a 3D hydrophobic barrier to separate the substrate from the aggressive dissolved oxygen and chloride ions. Meanwhile, owing to the thick protective layer and the release of excess 1-dodecanethiol molecules in the cavities, the film exhibited increased durability in the NaCl solution. The schematic is shown in Fig. 12.

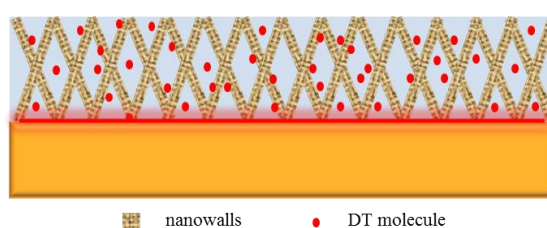


**Fig. 12** Schematic of networks on  $H_3PO_4$ -treated copper surface with 1-dodecanethiol SAMs

## 5. Conclusion

The corrosion resistance of 1-dodecanethiol SAMs on bare copper surface and copper surface treated with  $H_3PO_4$  solution was studied in 3.5% NaCl solution. 1-Dodecanethiol SAMs on both electrodes provide effective protection at the initial

time but gradually deteriorate in the subsequent 48 h. Notably, the corrosion rate values of H<sub>3</sub>PO<sub>4</sub>-treated copper with 1-dodecanethiol SAMs were one order of magnitude smaller than those of bare copper with 1-dodecanethiol SAMs. These results demonstrate that the 3D network constituted of Cu<sub>3</sub>(PO<sub>4</sub>)<sub>2</sub> nanoflower considerably improves the corrosion resistance of copper in NaCl solution when modified with 1-dodecanethiol SAMs.

### Author Contributions

Z.C conceived the work; S.H performed the experiments and wrote this paper; and X.G made valuable comments on this manuscript.

### Acknowledgment

The authors thank the National Natural Science Foundation of China (Nos. 51571098) for their financial support and the Analysis Support of the Analytical and Testing Center, Huazhong University of Science and Technology.

### Conflict of interest

The authors declare that the contents have no conflict of interest toward any individual or organization.

### Reference

1. Ho, H. M.; Lam, W.; Stoukatch, S.; Ratchev, P.; Vath III, C. J.; Beyne, E., Direct gold and copper wires bonding on copper. *Microelectronics Reliability* **2003**, *43*, (6), 913-923; DOI: 10.1016/S0026-2714(03)00074-X.
2. Finšgar, M.; Milošev, I., Inhibition of copper corrosion by 1, 2, 3-benzotriazole: a review. *Corrosion Science* **2010**, *52*, (9), 2737-2749; DOI:

- 10.1016/j.corsci.2010.05.002.
3. Zhang, D.-q.; Gao, L.-x.; Zhou, G.-d., Inhibition of copper corrosion in aerated hydrochloric acid solution by heterocyclic compounds containing a mercapto group. *Corrosion science* **2004**, 46, (12), 3031-3040; DOI: 10.1016/j.corsci.2004.04.012.
  4. Finšgar, M.; Merl, D. K., An electrochemical, long-term immersion, and XPS study of 2-mercaptobenzothiazole as a copper corrosion inhibitor in chloride solution. *Corrosion Science* **2014**, 83, 164-175; DOI: 10.1016/j.corsci.2014.02.016.
  5. Finšgar, M., 2-Mercaptobenzimidazole as a copper corrosion inhibitor: Part I. Long-term immersion, 3D-profilometry, and electrochemistry. *Corrosion Science* **2013**, 72, 82-89; DOI: 10.1016/j.corsci.2013.03.011.
  6. Kühnle, A., Self-assembly of organic molecules at metal surfaces. *Current Opinion in Colloid & Interface Science* **2009**, 14, (2), 157-168; DOI: 10.1016/j.cocis.2008.01.001
  7. Felhösi, I.; Kálmán, E.; Póczik, P., Corrosion protection by self-assembly. *Russian journal of electrochemistry* **2002**, 38, (3), 230-237; DOI: 10.1023/A:1014718320345.
  8. Laibinis, P. E.; Whitesides, G. M., Self-assembled monolayers of n-alkanethiolates on copper are barrier films that protect the metal against oxidation by air. *Journal of the American Chemical Society* **1992**, 114, (23), 9022-9028; DOI: 10.1021/ja00049a038.

9. Vikholm-Lundin, I.; Rosqvist, E.; Ihalainen, P.; Munter, T.; Honkimaa, A.; Marjomäki, V.; Albers, W. M.; Peltonen, J., Assembly of citrate gold nanoparticles on hydrophilic monolayers. *Applied Surface Science* **2016**, *378*, 519-529; DOI: 10.1016/j.apsusc.2016.03.213.
10. She, Z.; Di Falco, A.; Hähner, G.; Buck, M., Electrodeposition of gold templated by patterned thiol monolayers. *Applied Surface Science* **2016**, *373*, 51-60; DOI: 10.1016/j.apsusc.2015.12.054.
11. Yamamoto, Y.; Nishihara, H.; Aramaki, K., Self - Assembled Layers of Alkanethiols on Copper for Protection Against Corrosion. *Journal of the Electrochemical Society* **1993**, *140*, (2), 436-443; DOI: 10.1149/1.2221064.
12. Zhang, J.; Liu, Z.; Han, G.-C.; Chen, S.-L.; Chen, Z., Inhibition of copper corrosion by the formation of Schiff base self-assembled monolayers. *Applied Surface Science* **2016**, *389*, 601-608; DOI: 10.1016/j.apsusc.2016.07.116.
13. Zhang, X.; Liao, Q.; Nie, K.; Zhao, L.; Yang, D.; Yue, Z.; Ge, H.; Li, Y., Self-assembled monolayers formed by ammonium pyrrolidine dithiocarbamate on copper surfaces in sodium chloride solution. *Corrosion Science* **2015**, *93*, 201-210; DOI: 10.1016/j.apsusc.2016.07.116.
14. Itoh, M.; Nishihara, H.; Aramaki, K., Preparation and Evaluation of Two - Dimensional Polymer Films by Chemical Modification of an Alkanethiol Self - Assembled Monolayer for Protection of Copper Against Corrosion. *Journal of the Electrochemical Society* **1995**, *142*, (11), 3696-3704; DOI: 10.1149/1.2048401.

15. Yu, H.; Li, C.; Yuan, B.; Li, L.; Wang, C., The inhibitive effects of AC-treated mixed self-assembled monolayers on copper corrosion. *Corrosion Science* **2017**, 120, 231-238; DOI: 10.1016/j.corsci.2017.03.006.
16. Maho, A.; Denayer, J.; Delhalle, J.; Mekhalif, Z., Electro-assisted assembly of aliphatic thiol, dithiol and dithiocarboxylic acid monolayers on copper. *Electrochimica Acta* **2011**, 56, (11), 3954-3962; DOI: 10.1016/j.electacta.2011.02.020.
17. Wang, C.; Chen, S.; Zhao, S., Inhibition effect of AC-treated, mixed self-assembled film of phenylthiourea and 1-dodecanethiol on copper corrosion. *Journal of the Electrochemical Society* **2004**, 151, (1), B11-B15; DOI: 10.1149/1.1630595.
18. Rohwerder, M.; Stratmann, M., Surface modification by ordered monolayers: new ways of protecting materials against corrosion. *Mrs Bulletin* **1999**, 24, (7), 43-47; DOI: 10.1557/S0883769400052696.
19. Wang, J.; Ho, G. W., Corrosion - Mediated Self - Assembly (CMSA): Direct Writing Towards Sculpturing of 3D Tunable Functional Nanostructures. *Angewandte Chemie* **2015**, 127, (52), 16030-16034; DOI: 10.1002/ange.201509356.
20. He, G.; Hu, W.; Li, C. M., Spontaneous interfacial reaction between metallic copper and PBS to form cupric phosphate nanoflower and its enzyme hybrid with enhanced activity. *Colloids and Surfaces B: Biointerfaces* **2015**, 135, 613-618; DOI: 10.1016/j.colsurfb.2015.08.030.

21. Chen, S.; Chen, Y.; Lei, Y.; Yin, Y., Novel strategy in enhancing stability and corrosion resistance for hydrophobic functional films on copper surfaces. *Electrochemistry communications* **2009**, 11, (8), 1675-1679; DOI: 10.1016/j.elecom.2009.06.021.
22. Lee, M.-Y.; Ding, S.-J.; Wu, C.-C.; Peng, J.; Jiang, C.-T.; Chou, C.-C., Fabrication of nanostructured copper phosphate electrodes for the detection of  $\alpha$ -amino acids. *Sensors and Actuators B: Chemical* **2015**, 206, 584-591; DOI: 10.1016/j.snb.2014.09.106.
23. Wu, X.; Shi, G.; Wang, S.; Wu, P., Formation of 3D dandelions and 2D nanowalls of copper phosphate dihydrate on a copper surface and their conversion into a nanoporous CuO film. *European journal of inorganic chemistry* **2005**, 2005, (23), 4775-4779; DOI: 10.1002/ejic.200500413.
24. Hamada, S.; Kudo, Y.; Tojo, T., Preparation and reduction kinetics of uniform copper particles from copper (I) oxides with hydrogen. *Colloids and surfaces* **1992**, 67, 45-51; DOI: 10.1016/0166-6622(92)80284-9.
25. Lo, P. H.; Tsai, W. T.; Lee, J. T.; Hung, M. P., The Electrochemical Behavior of Electroless Plated Ni - P Alloys in Concentrated NaOH Solution. *Journal of the Electrochemical Society* **1995**, 142, (1), 91-96; DOI: 10.1149/1.2043954.
26. Wang, P.; Liang, C.; Wu, B.; Huang, N.; Li, J., Protection of copper corrosion by modification of dodecanethiol self-assembled monolayers prepared in aqueous micellar solution. *Electrochimica Acta* **2010**, 55, (3), 878-883; DOI: 10.1016/j.electacta.2009.06.078.

27. Ge, J.; Lei, J.; Zare, R. N., Protein–inorganic hybrid nanoflowers. *Nature nanotechnology* **2012**, 7, (7), 428; DOI: 10.1038/nnano.2012.80.
28. Frost, R. L.; Kloprogge, T.; Williams, P. A.; Martens, W.; Johnson, T. E.; Leverett, P., Vibrational spectroscopy of the basic copper phosphate minerals: pseudomalachite, ludjibaite and reichenbachite. *Spectrochimica Acta Part A: Molecular and Biomolecular Spectroscopy* **2002**, 58, (13), 2861-2868; DOI: 10.1016/S1386-1425(02)00034-3.
29. Laibinis, P. E.; Whitesides, G. M.; Allara, D. L.; Tao, Y. T.; Parikh, A. N.; Nuzzo, R. G., Comparison of the structures and wetting properties of self-assembled monolayers of n-alkanethiols on the coinage metal surfaces, copper, silver, and gold. *Journal of the American Chemical Society* **1991**, 113, (19), 7152-7167; DOI: 10.1021/ja00019a011.
30. Porter, M. D.; Bright, T. B.; Allara, D. L.; Chidsey, C. E., Spontaneously organized molecular assemblies. 4. Structural characterization of n-alkyl thiol monolayers on gold by optical ellipsometry, infrared spectroscopy, and electrochemistry. *Journal of the American Chemical Society* **1987**, 109, (12), 3559-3568; DOI: 10.1021/ja00246a011.
31. Bertilsson, L.; Liedberg, B., Infrared study of thiol monolayer assemblies on gold: preparation, characterization, and functionalization of mixed monolayers. *Langmuir* **1993**, 9, (1), 141-149; DOI: 10.1021/la00025a032.
32. Nakajima, A.; Hashimoto, K.; Watanabe, T., Recent studies on super-hydrophobic films. *Monatshefte für Chemie/Chemical Monthly* **2001**, 132,

- (1), 31-41; DOI: 10.1007/s007060170142.
33. Kear, G.; Barker, B.; Walsh, F., Electrochemical corrosion of unalloyed copper in chloride media—a critical review. *Corrosion science* **2004**, 46, (1), 109-135; DOI: 10.1016/S0010-938X(02)00257-3.
34. Feng, Y.; Siow, K.-S.; Teo, W.-K.; Tan, K.-L.; Hsieh, A.-K., Corrosion mechanisms and products of copper in aqueous solutions at various pH values. *Corrosion* **1997**, 53, (5), 389-398; DOI: 10.5006/1.3280482.
35. Deslouis, C.; Tribollet, B.; Mengoli, G.; Musiani, M. M., Electrochemical behaviour of copper in neutral aerated chloride solution. I. Steady-state investigation. *Journal of applied electrochemistry* **1988**, 18, (3), 374-383; DOI: 10.1007/BF01093751
36. Fiaud, C., Electrochemical Behaviour of Cu in Alkaline Solution and the Inhibitive Action of Cyclohexylamine. *Corrosion Sci.* **1974**, 14, (4), 261-277; DOI: 10.1016/S0010-938X(74)80036-3.
37. Abrantes, L.; Castillo, L.; Norman, C.; Peter, L., A photoelectrochemical study of the anodic oxidation of copper in alkaline solution. *Journal of electroanalytical chemistry and interfacial electrochemistry* **1984**, 163, (1-2), 209-221; DOI: 10.1016/S0022-0728(84)80053-4.
38. Li, S.; Wang, Y.; Chen, S.; Yu, R.; Lei, S.; Ma, H.; Liu, D. X., Some aspects of quantum chemical calculations for the study of Schiff base corrosion inhibitors on copper in NaCl solutions. *Corrosion Science* **1999**, 41, (9), 1769-1782; DOI: 10.1016/S0010-938X(99)00014-1.

39. Ma, H.; Yang, C.; Chen, S.; Jiao, Y.; Huang, S.; Li, D.; Luo, J., Electrochemical investigation of dynamic interfacial processes at 1-octadecanethiol-modified copper electrodes in halide-containing solutions. *Electrochimica acta* **2003**, 48, (28), 4277-4289; DOI: 10.1016/j.electacta.2003.08.003.
40. Brug, G.; Van Den Eeden, A.; Sluyters-Rehbach, M.; Sluyters, J., The analysis of electrode impedances complicated by the presence of a constant phase element. *Journal of electroanalytical chemistry and interfacial electrochemistry* **1984**, 176, (1-2), 275-295; DOI: 10.1016/S0022-0728(84)80324-1.
41. Metikoš-Huković, M.; Babić, R.; Petrović, Ž.; Posavec, D., Copper Protection by a Self-Assembled Monolayer of Alkanethiol Comparison with Benzotriazole. *Journal of the Electrochemical Society* **2007**, 154, (2), C138-C143; DOI: 10.1149/1.2404781.
42. Jennings, G. K.; Munro, J. C.; Yong, T.-H.; Laibinis, P. E., Effect of chain length on the protection of copper by n-alkanethiols. *Langmuir* **1998**, 14, (21), 6130-6139; DOI: 10.1021/la980333y.